

Optimising the integration of phase change materials in construction in South Mediterranean regions: A case study from Algiers, Algeria

Abdelkader Laafer¹, Abdelghani Yahiou², Thanina Hammouma^{1,3},

¹LTSM Laboratory, Mechanical Department, Faculty of Technology, Blida 1 University, 270 Soumaa Way Ouled Yaich, Blida, 09000, Algeria

²Electrical Engineering Department, Faculty of Applied Sciences, University of Bouira, 10000, Bouira, Algeria

³Sustainable Building Design Laboratory, Department of Urban and Environmental Engineering, Faculty of Applied Sciences, University of Liège, 4000, Liège, Belgium

ARTICLE INFO

ABSTRACT

Received: 28 Dec 2024

Revised: 18 June 2025

Accepted: 26 June 2025

This study investigates the integration of phase change materials (PCMs) into conventional building envelopes in Mediterranean climates, with a focus on Algiers, Algeria a region characterised by high diurnal temperature fluctuations and peak summer temperatures reaching 35 °C. The paraffin-based PCM RT35-HC (melting point ≈35 °C) was embedded at the core of wall assemblies composed of four locally prevalent construction materials: fired brick, aerated concrete, stabilised earth concrete, and slag concrete. Using COMSOL Multiphysics®, a two-dimensional transient heat transfer model was developed to evaluate the thermal performance of each wall configuration under representative climatic conditions. Simulations assessed the influence of material type and PCM placement on indoor thermal stability, particularly on time-lag, temperature attenuation, and heat flux reduction. Results indicate that aerated concrete combined with RT35-HC PCM provides the most effective thermal buffering, significantly delaying heat transfer and maintaining lower interior surface temperatures throughout the diurnal cycle. These findings support using PCM-enhanced lightweight materials to improve energy efficiency and thermal comfort in South Mediterranean regions.

Keywords: Paraffin RT35-HC, Thermal energy storage, Building envelope, Mediterranean Climate, Energy efficiency, Comsol Multiphysics, sustainable construction.

INTRODUCTION

The increase in energy consumption in the building sector is a major concern worldwide. Phase change materials (PCMs) offer a promising solution for improving the energy efficiency of buildings by storing latent heat and regulating indoor temperatures [1]. In particular, in hot regions where daytime temperatures can reach high levels, integrating PCMs into building structures can significantly reduce the thermal load and improve indoor thermal comfort [2,3].

PCMs, such as paraffins, are widely studied for their ability to absorb and release heat during phase transitions. RT35-HC PCM, for example, has been used effectively in various applications to stabilize indoor temperatures around 35°C [4]. Studies have shown that PCMs can reduce annual energy consumption by up to 22% in specific scenarios [5]. These materials are beneficial in environments where the demand for cooling is high, such as in hot and arid climates [6].

Current research focuses on optimising the thermal properties of PCMs and integrating them into various construction elements such as walls, roofs, and floors [7]. Advanced simulation software such as COMSOL Multiphysics makes it possible to assess the effectiveness of PCMs in various architectural configurations and climatic conditions [8]. These simulations help determine the optimum thickness and positioning of PCMs to maximise their thermal efficiency [9,10].

Despite the potential advantages of PCMs, a number of challenges remain with regard to their practical application. Selecting the right material for each specific climate [11] and managing material costs and durability are critical

factors to consider [1,3]. Further research is needed to develop cost-effective solutions that effectively integrate PCMs into buildings while minimising their environmental impact [12].

Integrating PCMs into the building sector represents a significant step towards a more sustainable future [13]. By optimising their use in hot regions such as Algiers in Algeria, it is possible to significantly reduce energy consumption while improving indoor thermal comfort [14]. This study explores these possibilities by using RT35-HC PCM with various local building materials to identify the most effective combinations [4].

This study's novelty is finding the ideal building material compatible with PCMs in general, specifically PCM RT35-HC in the arid climate, by finding the ideal melting point in hot 35-degree climatic conditions, including location and thickness. A numerical model of an embedded frame wall in thin-film PCM was created with several building materials in COMSOL Multiphysics® software and validated using experimental data.

OBJECTIVES

The study uses numerical simulation to assess the thermal efficiency of walls incorporating PCM RT35-HC. This material is a paraffin supplied by Rubitherm®, known for its phase transition around 35°C. Using four common construction materials, we modelled several wall configurations using brick, aerated concrete, stabilised earth concrete, and slag concrete. Each simulation was conducted under climatic conditions representing a typical day with a maximum outdoor temperature of 35°C.

METHODS

The PCM used is a paraffin called RT35-HC, supplied by the Rubitherm® company; it is an eicosane (alkane with 20 carbon atoms), whose phase transitions around 35°C. To determine its thermophysical properties [15], PCM was characterised by DSC, using a μ DSC7evo calorimeter. The apparent heat capacity curves measured are plotted in Figure 1 [15]. The peak observed around 32°C in single solidification corresponds to a solid-solid phase transition; with the exception of this peak, the curves are the same in melting and solidification. The phase change enthalpy was estimated graphically (tangent method) from the curve measured during melting, then recalibrated to obtain the same melting time under load in the simulation as in the experiment. The value adopted (246 kJ.kg⁻¹) is consistent with the uncertainty given by the supplier, and with other measurements carried out on eicosane. The values adopted for the properties of MCP are listed in Table 1. [16,17]

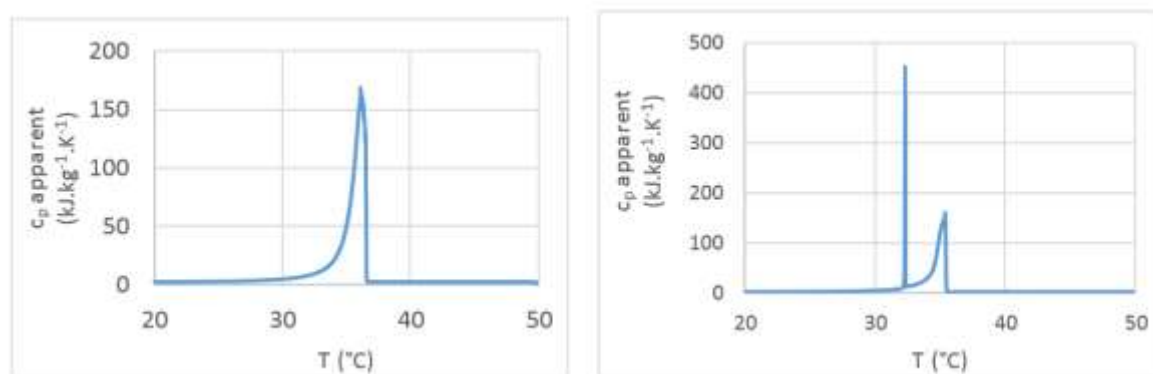


Figure 1: Apparent heat capacity of RT35-HC measured by DSC (0.01 K/min)[15]

This figure shows the apparent heat capacity of MCP RT35-HC during the melting and solidification processes. The peak observed indicates a solid-solid phase transition around 32°C.

The consistency between the melting and solidification curves suggests that MCP has good potential to stabilize internal temperatures by efficiently storing and releasing latent heat.



Figure 3: Case Study orientation [18]

Building materials

In this study, we focused on the four materials most commonly used in the Mediterranean region of Algeria.

Brick

Bricks are generally rectangular parallelepiped-shaped building elements made from raw clay, either sun-dried or kiln-fired. Bricks can be used to build walls, and their manufacture can vary depending on the region and the techniques used.

Cellular Concrete

Cellular concrete is a lightweight, insulating building material made mainly of water, sand, cement, lime and a blowing agent such as aluminium powder. It is manufactured in such a way as to create cells that make it light and give it excellent thermal and acoustic insulation properties. The material is non-flammable, easy to handle and does not require additional insulation. However, it can be brittle and requires care when cutting and fixing objects. Aerated concrete is widely used for walls, partitions, ceilings and other structural elements, offering ecological and practical advantages [19].

Stabilised Earth Concrete

Stabilised earth concrete is a construction material that uses natural ingredients, mainly clay, sand, gravel, and water, but it adds stabilisers to improve its mechanical properties and durability. These stabilisers can include Portland cement, lime, slag, vegetable reinforcement, asphalt, coconut oil, and chemical treatments to ensure waterproofing and chemical stability. The added stabilisers improve the material's mechanical strength, cohesion, and durability by reducing porosity, permeability, and swelling and increasing compressive, tensile, and shear strength [1].

Slag Concrete

Slag concrete is a type of hydraulic concrete that uses slag, a solid residue from the smelting of iron ore with coke in blast furnaces, as its main material. Slag is composed of lime, alumina and silica, and has hydraulic properties similar to those of clinker. When cooled suddenly, slag hydrates more slowly but is more stable in aggressive environments [20].

Numerical Model

A 2D transient heat conduction model was developed in COMSOL Multiphysics® (Heat Transfer Module), presented in Figures 4 and 5. The wall was modelled as a multi-layered vertical slab (1 m height × total thickness per material), with the PCM layer (5 mm) embedded at the geometric centre to maximise thermal buffering (Figure 6).

Heat equation

The heat equation is a parabolic partial differential equation introduced in the early 19th century by Fourier to describe the physical phenomenon of heat conduction [21].

Let be a domain of \mathbb{R}^3 with boundary $\Gamma = \partial$ and $T(x, t)$ a temperature field on this domain (field of scalars). In the presence of a thermal source in the domain, and in the absence of convection, i.e. heat transport (i.e. we are interested in the propagation of temperature within a 'stable' medium, i.e. one that does not move; we are not interested in the propagation of heat due, for example, to the existence of an air current, a convection current. Convection is more of a fluid mechanics problem.

The heat equation is written as:

$$\rho c \frac{\partial T}{\partial t} = \nabla \cdot (D \nabla T) + f \quad (1)$$

Where:

∇ is the Laplacian operator.

D is the thermal diffusivity coefficient (in m^2/s).

f is the volume heat output (in W / m^3).

ρ is the density of the material (in kg / m^3).

c is the mass-specific heat of the material (in $\text{J}/\text{kg.K}$).

The heat equation is therefore of the form:

$$-\Delta u = f \quad (2)$$

It is parabolic. For the problem to be posed appropriately, we need to specify: an initial condition:

$$T(x, 0) = T_0(x) \quad (3)$$

A boundary condition on the edge of the domain, for example: Dirichlet:

$$T(x, 0) = 0 \quad (4)$$

Neumann:

$$\frac{\partial T}{\partial n} = 0 \quad (5)$$

Where $n(x)$ is the unit normal vector at point x . The heat equation, initially introduced to describe heat conduction, can be used to describe the phenomenon of diffusion. Diffusion is an irreversible transport phenomenon that eventually results in a homogenisation of the quantity under consideration (e.g. the temperature in a field, the concentration of chemicals in a solution, etc.). From a phenomenological point of view, and to first order, this phenomenon is governed by Fick's law (e.g. water sorption in composite materials, diffusion of active ingredients through the skin). In the above equation, T represents the distribution of the quantity under consideration (water in a composite, concentration of a chemical constituent, etc.) and the source term in Ω is often zero (i.e. $f = 0$).

sensible and latent heat equation

$$Q = mC_p(T_f - T_i) \quad (7)$$

$$Q = m \underbrace{[C_{sp}(T_m - T_i) + C_{lp}(T_f - T_m)]}_{\text{Sensible heat energy}} + \underbrace{a_m \Delta h_m}_{\text{Latent heat energy}} \quad (8)$$

Using the equation below, the COMSOL Multiphysics® software considers the dynamics of the phase change process from phase I (solid) to phase II (liquid) in PCM.

$$\rho_{PCM} = \rho_{Phase1}\beta + \rho_{Phase2}(1 - \beta) \quad (9)$$

$$\lambda_{PCM} = \lambda_{Phase1}\beta + \lambda_{Phase2}(1 - \beta) \quad (10)$$

$$C_{p,PCM} = \frac{1}{\rho_{PCM}} \left(\rho_{Phase1} C_{p,Phase1} \beta + \rho_{Phase2} C_{p,Phase2} (1 - \beta) \right) + L \frac{\partial \alpha_m}{\partial T} \quad (11)$$

C_p: specific heat (J/kg.K).

L: latent heat of fusion (J/kg).

Since PCM is assumed to have the same thermal conductivity in the solid and liquid phases, equation 6b can be rewritten as follows:

$$\lambda_{PCM} = \lambda_{Phase1} = \lambda_{Phase2} \quad (12)$$

And α_m is :

$$\alpha_m = \frac{1}{2} \frac{\rho_{Phase2}(1-\beta) - \rho_{Phase1}\beta}{\rho_{Phase2}(1-\beta) + \rho_{Phase1}\beta} \quad (13)$$

β : the volume fraction of PCM in the initial phase 1 (solid).

α_m : represents the mass percentage of PCM transferred from phase 1 to phase 2.

Boundary conditions

To solve PDEs, it is necessary to define a number of consistent boundary conditions. Each domain surface has an associated oriented segment. It is possible to give boundary condition values for each of these segments. The options will differ depending on whether or not the surface is internal to the system. Let's choose the different boundary conditions appropriately.



Figure 4: The internal face of the case study room

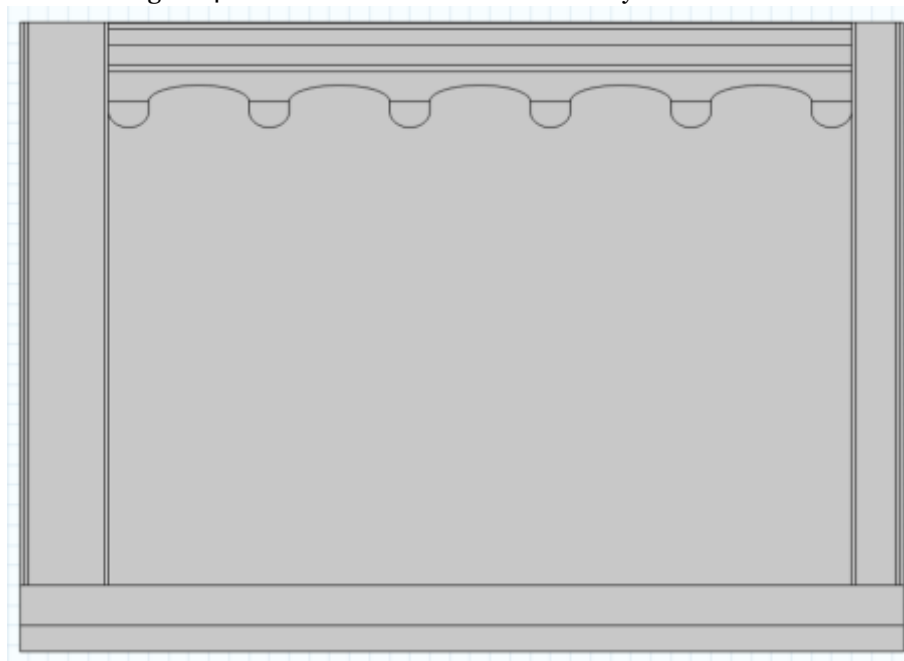


Figure 5: The model building of the case study on 2D

The mesh

The mesh corresponds to the spatial discretisation of the geometry into elementary volumes (meshes) defined by nodes. These nodes form the connections between the meshes. The software creates the mesh automatically. The algorithm takes the elements of the geometry as its starting point. It creates additional nodes until it satisfies predefined criteria, such as the number of meshes or the maximum mesh size. You can use the sizes predefined (extra coarse, coarse, normal, fine, extra fine, etc.) by the software or act on the mesh generation parameters.

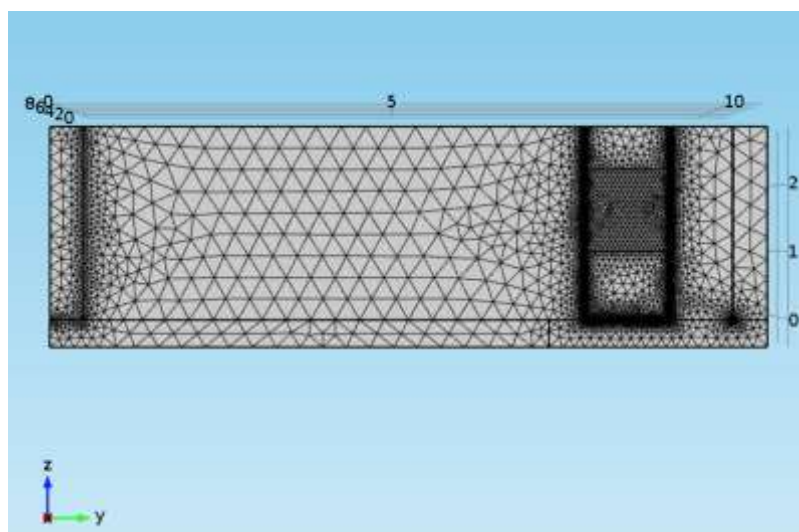


Figure 6: The Mesh of the case study for the external side.

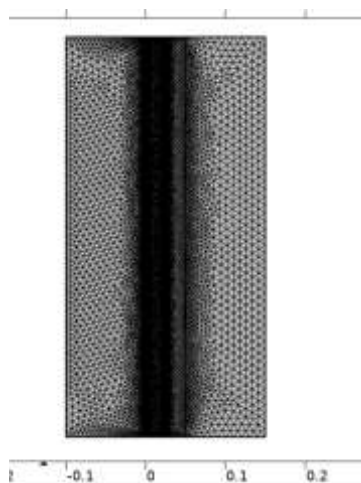


Figure 7: Definition of the Mesh in the external wall.

The mesh size used is crucial to the accuracy of the thermal simulations. A fine mesh allows accurate modelling of thermal gradients in materials, which is essential for comparing the thermal performance of different building materials.

Validation Model

Simulation results were validated with the same experimental values confirmed by a.lafer et al[18], for 60 hours of simulation using RMSD and MAE Methods. The experimental and theoretical temperature profiles confirm the agreement between the two data sets. The maximum and average deviations between experimental and numerical values were 0.75% and 0.35%, respectively.

RESULTS

Resolution procedure

The numerical model was constructed using a physics-controlled 2D sequential mesh with an extra-fine element size (Figure 7). Each domain was discretized using free tetrahedral elements, forming a non-structural and linear mesh in the boundaries between layers. The grid cell has a mesh of 291107 nodes and 24089 internal boundaries, with a simulation time step of 30 minutes. The simulation duration was approximately 2 hours, 4 minutes, and 33 seconds. The simulation was carried out on a Macintosh computer equipped with a 4th-generation quad-core i7 processor at

2.0 GHz, boosted to 3.2 GHz during the calculation, with 8 GB of RAM. This was further increased to 64 GB when calculating using an SSD hard disk and a 2 GHz Iris Pro graphics card.

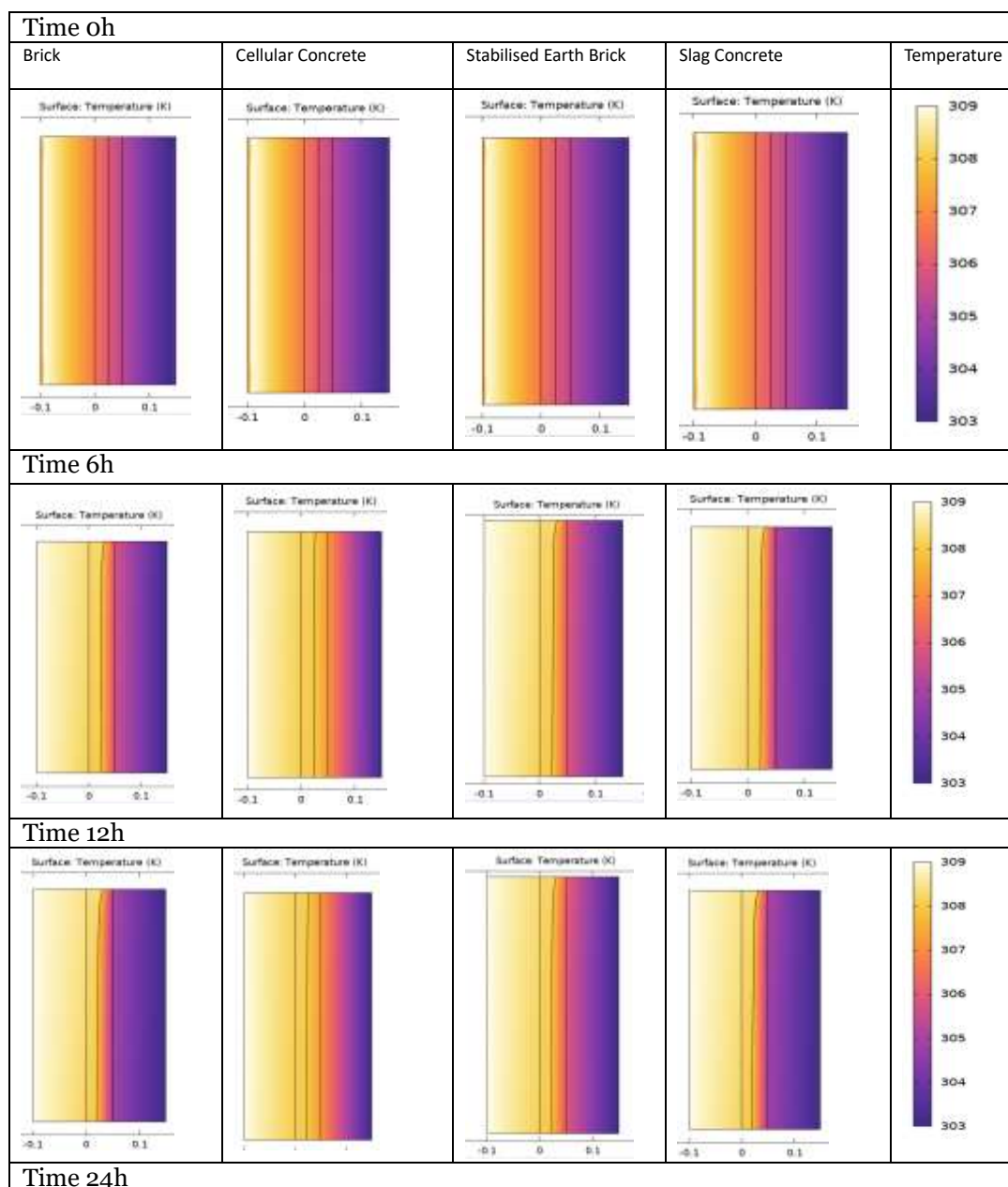
Simulation results

The following graphs show the simulation results for a complete day. The wall is between two different temperatures, external 35°C and internal 30°C.

Temperature (ht)

Wall temperature change as a function of time

The figure illustrates the temperature distribution in walls built with different materials at different times of day.



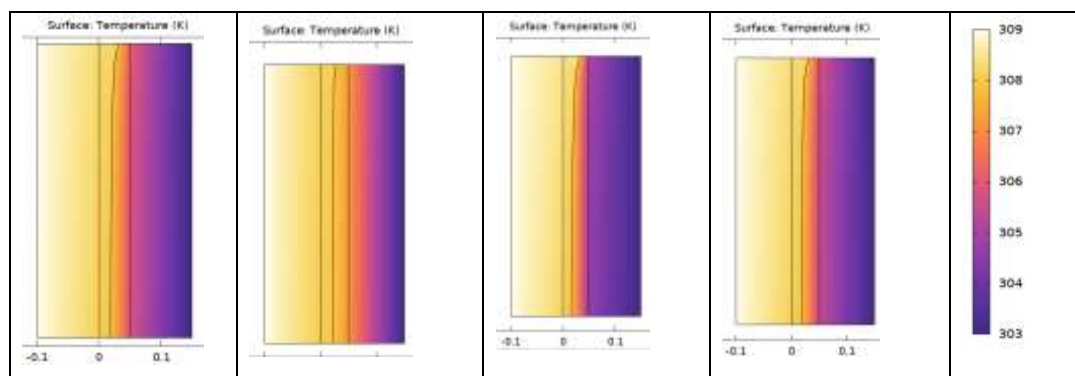


Figure 8: The temperature distribution in walls built with different materials at different times of day

At $t = 0$ h

All wall configurations exhibit a uniform initial temperature of 30 °C on the inside face of the building (interior wall), confirming consistent thermal equilibrium before external heating. This homogeneous starting condition ensures a fair comparative assessment of material-specific thermal responses under identical boundary conditions.

At $t = 6$ h

Stabilised earth concrete demonstrates superior early-stage thermal regulation, with slower heat propagation toward the interior than brick and slag concrete. Although cellular concrete exhibits low thermal conductivity, its very light structure limits thermal inertia, resulting in less effective buffering during the initial heating phase. In contrast, stabilised earth combining natural aggregates with cementitious stabilisers provides a balanced thermal response, delaying heat transfer while preparing the PCM for optimal activation.

At $t = 12$ h

At midday, when the external temperature reaches 35 °C, stabilised earth concrete maintains the lowest interior surface temperature among all configurations. The PCM layer (center) shows a pronounced isothermal plateau near 35 °C, confirming efficient latent heat absorption. This indicates that the material's moderate thermal conductivity ($\sim 0.6\text{--}0.8$ W/m·K) allows controlled heat flux that matches the PCM's phase-change capacity, unlike cellular concrete, where excessive insulation delays PCM activation, reducing its effectiveness during peak hours.

At $t = 24$ h

Stabilised earth brick exhibits excellent thermal stability by the end of the 24-hour cycle, with the smallest diurnal temperature swing at the interior surface. This confirms its superior thermal time-lag and decrement factor, critical for passive cooling in Ghardaïa's arid climate with significant day-night temperature differences. The material's ability to combine sensible heat storage (from its mineral matrix) with latent heat buffering (from PCM) creates a synergistic thermal regulation mechanism unmatched by purely insulating (cellular) or highly conductive (brick, slag) alternatives.

DISCUSSION

Temperature graphs at several points

These figures show how the temperature evolves as a function of time at several specific points on the wall.

Each point represents a strategic location in the wall for observing thermal gradients.

These figures show how the temperature changes at different wall points built with various materials combined with the RT35-HC PCM. Each figure focuses on a specific point in the wall, allowing the differences in thermal performance between materials to be observed.

Point 1

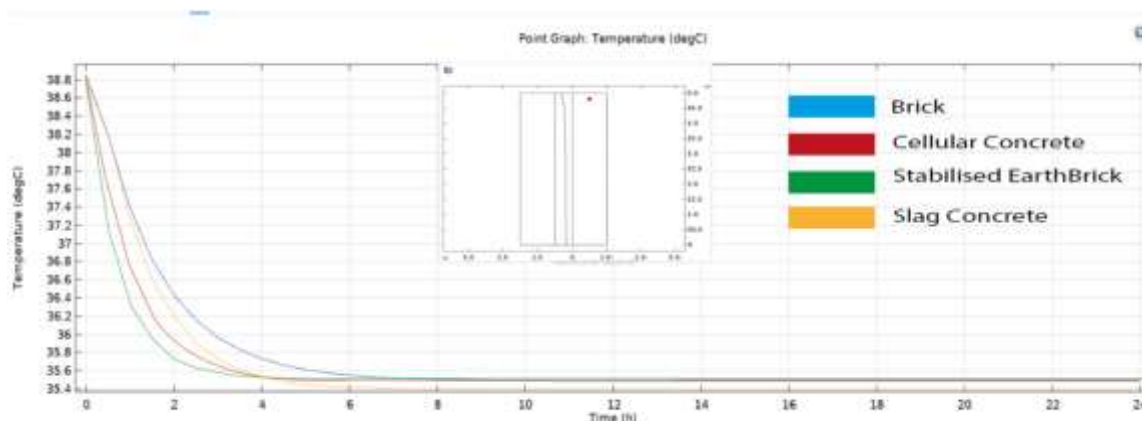


Figure 9: Exterior Surface (Exposed to 35°C Ambient)

All wall configurations exhibit nearly identical thermal responses at the exterior surface, following the imposed boundary condition of a 35 °C peak temperature presented in Figure 9. This uniformity confirms that the external thermal loading was consistently applied across all simulations, ensuring a fair comparative assessment of material-specific performance. Minor deviations are negligible and attributable to slight differences in surface emissivity or thermal effusivity, which do not affect the overall validity of the comparison.

Point 2

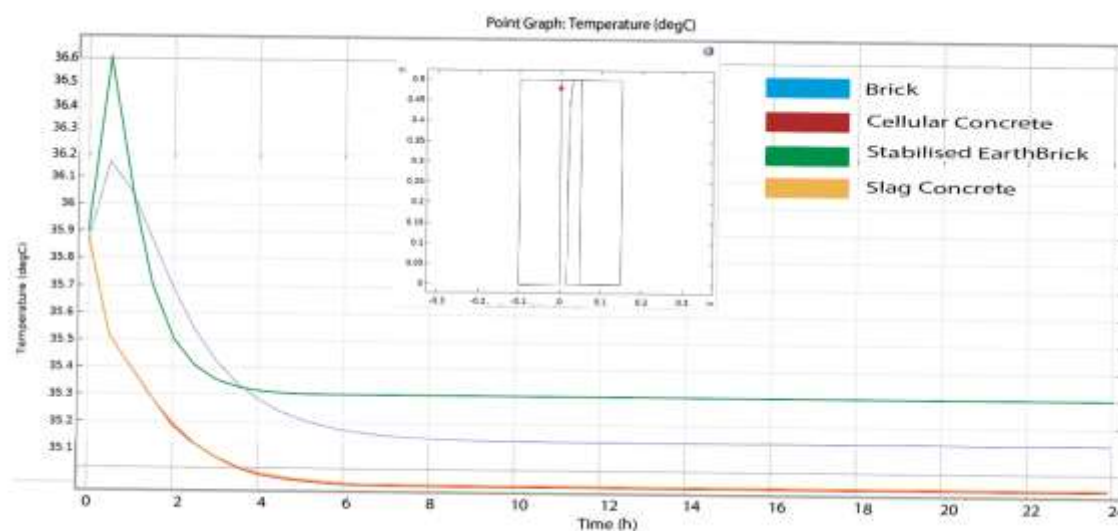


Figure 10: Wall Core (Location of RT35-HC PCM Layer)

The temperature evolution at the PCM interface reveals critical differences in latent heat utilisation. In Stabilized EarthBrick, the temperature rises gradually and plateaus near 35 °C for an extended duration (approximately 5–6 hours around midday), indicating efficient and sustained melting of the RT35-HC PCM (Figure 10). This prolonged phase-change period demonstrates optimal synergy between the PCM and the low-conductivity matrix. This slows heat ingress and fully exploits the material's 246 kJ/kg latent heat capacity.

In contrast, due to their higher thermal conductivity, brick, slag concrete, and cellular concrete exhibit sharper, shorter peaks at this point, suggesting that heat flux overwhelms the PCM, limiting its ability to absorb latent heat effectively. The PCM in these materials transitions too rapidly, reducing its thermal buffering potential.

Point 3

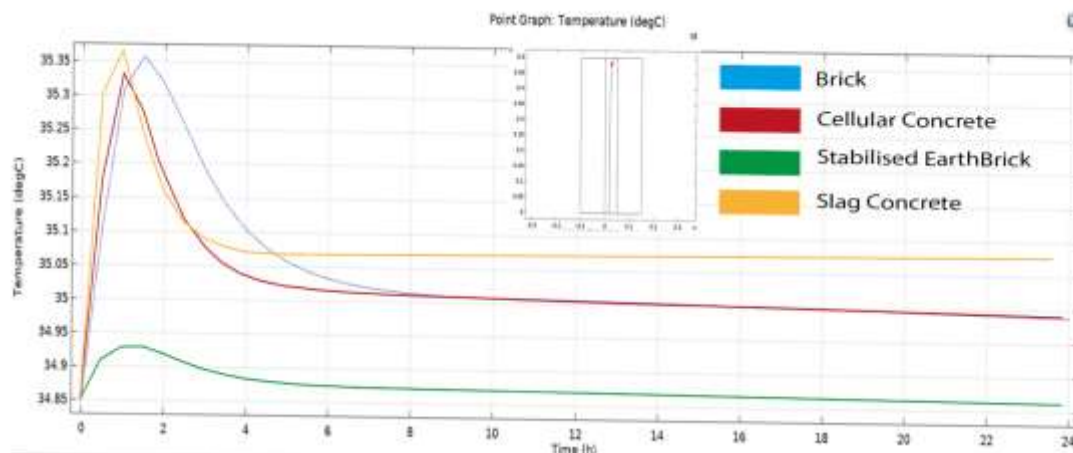


Figure 11: Interior Surface (Indoor Side, Facing 30°C Environment)

This point, directly presented in Figure 11, reflects indoor thermal comfort and passive cooling performance. Stabilised earth brick + RT35-HC achieves the lowest peak temperature and the smallest diurnal fluctuation among all configurations. At $t = 12$ h, while other materials show significant heat penetration, BTS maintains a stable interior surface close to the initial 30 °C. By $t = 24$ h, it continues outperforming all alternatives, confirming its superior thermal time-lag and decrement factor.

These results demonstrate that low thermal conductivity combined with PCM integration provides the most effective strategy for attenuating heat transfer in Mediterranean climates, where minimizing indoor temperature swings is essential for thermal comfort in naturally ventilated buildings.

CONCLUSION

This study investigated the integration of RT35-HC phase change material into four locally prevalent wall materials in Algiers, Algeria, a representative Mediterranean region with summer temperatures reaching 35 °C. Contrary to conventional assumptions that prioritise low-conductivity materials, stabilised earth brick emerged as the most effective host matrix for PCM integration. Its balanced thermophysical properties moderate thermal conductivity, sufficient volumetric heat capacity, and compatibility with local construction practices enable optimal synchronisation between conductive heat flow and PCM phase change. This synergy results in superior interior temperature stability, extended thermal time-lag, and enhanced passive cooling potential compared to cellular concrete, fired brick, and slag concrete.

The findings highlight that maximising PCM performance requires more than just insulation; it demands a strategic balance between thermal mass and resistance. Given that stabilised earth concrete is locally available, low-cost, and sustainable, its combination with RT35-HC offers a practical, scalable solution for improving energy efficiency and thermal comfort in arid regions. Future work will focus on experimental validation, long-term durability under real climatic conditions, and life-cycle assessment to support policy integration in sustainable building codes.

ACKNOWLEDGEMENT

The authors would like to thank Zakaria Guicheniti and Mohamed Slimane Touati for their suggestions during the preparation and writing of this article.

REFERENCES

- [1] M. Kadri, A. Bouchair, and A. Laafer, “The contribution of double skin roof coupled with thermo reflective paint to improve thermal and energy performance for the “Mozabit” houses: Case of Beni Isguen’s Ksar in southern Algeria,” *Energy Build.*, vol. 256, p. 111746, Feb. 2022, doi: 10.1016/j.enbuild.2021.111746.

- [2] H. Zhan, N. Mahyuddin, R. Sulaiman, and F. Khayatian, "Phase change material (PCM) integrations into buildings in hot climates with simulation access for energy performance and thermal comfort: A review," *Constr. Build. Mater.*, vol. 397, p. 132312, Sept. 2023, doi: 10.1016/j.conbuildmat.2023.132312.
- [3] M. Ahangari and M. Maerefat, "An innovative PCM system for thermal comfort improvement and energy demand reduction in building under different climate conditions," *Sustain. Cities Soc.*, vol. 44, pp. 120–129, Jan. 2019, doi: 10.1016/j.scs.2018.09.008.
- [4] H. F. Öztö, E. Gürgeç, and M. Gür, "Thermophysical properties and enhancement behavior of novel B4C-nanoadditive RT35HC nanocomposite phase change materials: Structural, morphological, thermal energy storage and thermal stability," *Sol. Energy Mater. Sol. Cells*, vol. 272, p. 112909, Aug. 2024, doi: 10.1016/j.solmat.2024.112909.
- [5] R. Kalbasi, "Usefulness of PCM in building applications focusing on envelope heat exchange – Energy saving considering two scenarios," *Sustain. Energy Technol. Assess.*, vol. 50, p. 101848, Mar. 2022, doi: 10.1016/j.seta.2021.101848.
- [6] M. A. Wahid, S. E. Hosseini, H. M. Hussien, H. J. Akeiber, S. N. Saud, and A. Th. Mohammad, "An overview of phase change materials for construction architecture thermal management in hot and dry climate region," *Appl. Therm. Eng.*, vol. 112, pp. 1240–1259, Feb. 2017, doi: 10.1016/j.applthermaleng.2016.07.032.
- [7] S. Dardouri, E. Tunçbilek, O. Khaldi, M. Arıcı, and J. Sghaier, "Optimizing PCM Integrated Wall and Roof for Energy Saving in Building under Various Climatic Conditions of Mediterranean Region," *Buildings*, vol. 13, no. 3, p. 806, Mar. 2023, doi: 10.3390/buildings13030806.
- [8] R. M. Ismail, N. A. Megahed, and S. Eltarabily, "Numerical investigation of the indoor thermal behaviour based on PCMs in a hot climate," *Archit. Sci. Rev.*, vol. 65, no. 3, pp. 196–216, May 2022, doi: 10.1080/00038628.2022.2058459.
- [9] M. Aadmi, M. Karkri, and M. El Hammouti, "Heat transfer characteristics of thermal energy storage for PCM (phase change material) melting in horizontal tube: Numerical and experimental investigations," *Energy*, vol. 85, pp. 339–352, June 2015, doi: 10.1016/j.energy.2015.03.085.
- [10] M. Li, Q. Cao, H. Pan, X. Wang, and Z. Lin, "Effect of melting point on thermodynamics of thin PCM reinforced residential frame walls in different climate zones," *Appl. Therm. Eng.*, vol. 188, p. 116615, Apr. 2021, doi: 10.1016/j.applthermaleng.2021.116615.
- [11] F. Souayfane, F. Fardoun, and P.-H. Biwole, "Phase change materials (PCM) for cooling applications in buildings: A review," *Energy Build.*, vol. 129, pp. 396–431, Oct. 2016, doi: 10.1016/j.enbuild.2016.04.006.
- [12] K. Saafi and N. Daouas, "Energy and cost efficiency of phase change materials integrated in building envelopes under Tunisia Mediterranean climate," *Energy*, vol. 187, p. 115987, Nov. 2019, doi: 10.1016/j.energy.2019.115987.
- [13] X. Wang, W. Li, Z. Luo, K. Wang, and S. P. Shah, "A critical review on phase change materials (PCM) for sustainable and energy efficient building: Design, characteristic, performance and application," *Energy Build.*, vol. 260, p. 111923, Apr. 2022, doi: 10.1016/j.enbuild.2022.111923.
- [14] A. Tellache, Y. Lazri, A. Laafer, and S. AttiaA., "Development of a Benchmark Model for Residential Buildings with a Mediterranean Climate: The Aero-Habitat in Algiers City" *Sustainability* 2025, 17(3), 831; <https://doi.org/10.3390/su17030831>
- [15] C. Beust, J.-P. Bedecarrats, and J. Pouvreau, "Influence des paramètres de modélisation sur la simulation numérique d'un module de stockage thermique par chaleur latente avec ailettes circulaires," p. 8, 2018.
- [16] M. Martinelli, "Stockage d'énergie thermique par changement de phase – Application aux réseaux de chaleur," phdthesis, Université Grenoble Alpes, 2016. Accessed: Oct. 26, 2024. [Online]. Available: <https://theses.hal.science/tel-01412771>
- [17] C. Vélez, M. Khayet, and J. M. Ortiz De Zárate, "Temperature-dependent thermal properties of solid/liquid phase change even-numbered n-alkanes: n-Hexadecane, n-octadecane and n-eicosane," *Appl. Energy*, vol. 143, pp. 383–394, Apr. 2015, doi: 10.1016/j.apenergy.2015.01.054.
- [18] A. Laafer, D. Semmar, A. Hamid, and M. Bourouis, "Thermal and Surface Radiosity Analysis of an Underfloor Heating System in a Bioclimatic Habitat," *Energies*, vol. 14, no. 13, p. 3880, June 2021, doi: 10.3390/en14133880.

- [19] L. Chica and A. Alzate, "Cellular concrete review: New trends for application in construction," *Constr. Build. Mater.*, vol. 200, pp. 637–647, Mar. 2019, doi: 10.1016/j.conbuildmat.2018.12.136.
- [20] I. Amer, M. Kohail, M. S. El-Feky, A. Rashad, and M. A. Khalaf, "A review on alkali-activated slag concrete," *Ain Shams Eng. J.*, vol. 12, no. 2, pp. 1475–1499, June 2021, doi: 10.1016/j.asej.2020.12.003.
- [21] G. Ruocco, "Heat Transfer by Conduction," in *Introduction to Transport Phenomena Modeling: A Multiphysics, General Equation-Based Approach*, G. Ruocco, Ed., Cham: Springer International Publishing, 2018, pp. 13–66. doi: 10.1007/978-3-319-66822-2_2.
- [22] F. Opoku, M. N. Uddin, and M. Atkinson, "A review of computational methods for studying oscillating water columns – the Navier-Stokes based equation approach," *Renew. Sustain. Energy Rev.*, vol. 174, p. 113124, Mar. 2023, doi: 10.1016/j.rser.2022.113124.